

Surface modification of ZrO₂ nanopowder with oxovanadium species using slurry deposition and impregnation methods

A. Adamski^{a,*}, P. Zapała^a, P. Jakubus^b, Z. Sojka^a

^a Faculty of Chemistry and Regional Laboratory of Physicochemical Analyses and Structural Research, Jagiellonian University, Ingardena 3, 30-060 Krakow, Poland

^b Institute of Chemistry and Environment Protection, Szczecin Technical University, Al. Piastów 42, 71-065 Szczecin, Poland

Received 17 June 2006; received in revised form 30 June 2006; accepted 14 July 2006

Available online 30 January 2007

Abstract

Structural differences in zirconia-supported vanadia, containing 3 mol% V₂O₅, obtained by slurry deposition and wet impregnation were elucidated using Raman, EPR and XRD methods, supported by Rietveld refinement. The preparation method strongly determines both the heterogeneity of the surface VO_x species and incorporation of the V⁴⁺ ions into the zirconia matrix. Slurry deposition favors the formation of isolated or two-dimensional oxovanadium clusters, whereas impregnation leads to agglomerated nanocrystalline V₂O₅. The stability of surface vanadium was discussed in terms of its reducibility and changes in the temperature of the tetragonal to monoclinic ZrO₂ phase transition, induced by surface doping.

© 2007 Elsevier B.V. All rights reserved.

PACS: 61.66.-f; 81.05.-t; 81.16 Be; 81.07 Wx

Keywords: Oxide materials; Chemical synthesis; Slurry deposition; Impregnation; Vanadium ions speciation

1. Introduction

Influence of the preparation method on the structure and properties of composed nano-oxide materials is one of the most important factors for tailoring them toward specific applications [1]. For example, considering a two-component supported system, where the major oxide plays the role of carrier, whereas the minor one is a deposited functional phase (*e.g.*, supported catalysts, chemical oxide sensors), dispersion of the deposited oxide, heterogeneity of surface entities and dissolution of the additive ions in the bulk, are strongly determined by the preparation method and the treatment conditions as well.

Classic impregnation is one of the most popular methods of deposition of one oxide onto another. This term denotes a procedure, where an excessive volume of the precursor solution is contacted the carrier [2]. Slurry deposition is a more recent preparation procedure, where practically insoluble oxide, functioning as a support, is mixed with the slurry of a poorly soluble

oxide to be deposited [3]. So far such procedure was used for synthesis of supported MoO₃ materials [4]. In this work, we adapted this procedure for spreading V₂O₅ on the surface of the tetragonal ZrO₂ nanopowder.

2. Experimental

Single-phase tetragonal ZrO₂ support (*t*-ZrO₂) of enhanced thermal stability was obtained by modified precipitation method from aqueous solutions of 0.6 M ZrOCl₂·8H₂O (Aldrich 99.99%) with 25% aqueous solution of ammonia [5]. VO_x/ZrO₂ samples, containing nominally 3 mol% of V₂O₅, were prepared by impregnation of the *t*-ZrO₂ matrix with an aqueous solution of NH₄VO₃ (99%, Merck) and by deposition from a slurry consisting of 0.1455 g of V₂O₅ (99.6%, Merck) in 5 cm³ of water at 353–373 K. These samples are denoted as *imp*-VO_x/ZrO₂ and *sdp*-VO_x/ZrO₂, respectively. All samples were dried at 373 K for 12 h. The impregnated samples were calcined in air at 873 K for 6 h.

The X-ray diffraction patterns were recorded by means of a DRON-3 (Bourestnik, Russia) and a Philips PW 1820 diffractometers, equipped with Fe and Ni filters, respectively, using Co K_α and Cu K_α radiations. For Rietveld refinement (using the DBWS-9411 program [6]), the 2 θ scans were carried out in 0.02° steps. High-resolution transmission electron microscopy (HR-TEM) was carried out using a JEM-100CX II UHR instrument (JEOL) operating at 100 kV. Raman spectra were collected on a FTS 6000 spectrometer equipped with a BIORAD accessory. The samples were excited with the 1064 nm line of a diode-pumped Nd:YAG laser (Spectra Physics Model T108S) and the scattered

* Corresponding author. Tel.: +48 12 663 22 24; fax: +48 12 634 05 15.
E-mail address: adamski@chemia.uj.edu.pl (A. Adamski).

radiation was collected at 180° with 4 cm^{-1} resolution. The CW-EPR X-band spectra were recorded at 77 K with a Bruker ELEXYS E-500 spectrometer, operating at the 100 kHz field modulation. The spectra simulation was performed using the EPRsim32 program [7]. The samples were heated *ex situ*, with the rate of 4 K/min, from room temperature to 1273 K in 100 K steps, and then kept for 0.5 h at each temperature, before measurement of the EPR spectra.

3. Results and discussion

The XRD patterns recorded in the range of $10\text{--}70^\circ$ for the *sdp*- VO_x/ZrO_2 and the *imp*- VO_x/ZrO_2 dry samples are typical of *t*- ZrO_2 polymorph. An intense maximum centered at 35° can be ascribed to (1 1 1) reflection of the tetragonal phase, whereas weak maxima at 41° and 59° to (2 0 0)/(0 0 2) and (0 2 2)/(2 2 0) reflections of *t*- ZrO_2 , respectively [8,9]. No traces of the monoclinic zirconia (*m*- ZrO_2) with the diagnostic (1 1 1) and (1 1 $\bar{1}$) reflections, could be observed. The average size of particles, assessed from the Scherrer analysis of the XRD line widths, was equal to $6.360 \pm 0.024\text{ nm}$. This remains in accordance with the size of tetragonal nanodomains, determined in parallel HR-TEM studies [5].

The absence of any reflections from V_2O_5 nanocrystals implies the lack of an extended aggregation of the deposited vanadia. Heating of the samples till 873 K did not lead to any distinct changes in the diffractograms, confirming relatively good thermal stability of *t*- ZrO_2 in the presence of 3 mol% of vanadia. However, Raman spectra (Fig. 1) exhibited distinct difference between the *imp*- VO_x/ZrO_2 and *sdp*- VO_x/ZrO_2 samples, in the range below 700 cm^{-1} , where the lattice vibrations of the support appear [10,11]. The factor group theoretical analysis predicts six Raman active modes ($A_{1g} + 2B_{1g} + 3E_g$) for the tetragonal form and 18 ($9A_g + 9B_g$) active modes for the monoclinic ZrO_2 [12]. Careful inspection of the deconvoluted diagnostic fragments of both spectra, revealed a small contribution of *m*- ZrO_2 to the *imp*- VO_x/ZrO_2 sample. Apart from intense bands characteristic of *t*- ZrO_2 at 148 cm^{-1} (B_{1g}), 266 cm^{-1} (E_g), 316 cm^{-1} (B_{1g}), 450 cm^{-1} (E_g), 645 cm^{-1} (E_g), domi-

nating both spectra, also weak bands from *m*- ZrO_2 at 191 cm^{-1} (A_g), 375 cm^{-1} (B_g) and 476 cm^{-1} (A_g) can be found in the Raman spectrum of *imp*- VO_x/ZrO_2 (Fig. 1a). The observed partial destabilization of the metastable *t*- ZrO_2 is thus, apparently induced by the interaction with V_2O_5 , produced on the support surface upon the calcination [13].

The main bands of oxovanadium species present on the zirconia surface can be clearly observed in the Raman spectra above 700 cm^{-1} . Strong bands at 777 cm^{-1} and 991 cm^{-1} , dominating the spectrum of *imp*- VO_x/ZrO_2 (Fig. 1a) and a weak band at *ca.* 990 cm^{-1} in the spectrum of *sdp*- VO_x/ZrO_2 (Fig. 1b), reflect significant differences in the vanadium dispersion in both samples. The band at 777 cm^{-1} can be ascribed to $\nu_{\text{V-O-V}}$ mode (B_{3u}) in three-dimensional V_2O_5 nanocrystallites [14]. The band around 990 cm^{-1} is characteristic of a symmetrical $\nu_{\text{V=O}}$ mode in a variety of the octahedral oxovanadium species [15,16]. In case of the *imp*- VO_x/ZrO_2 sample, only the presence of a well crystalline nano- V_2O_5 entities can explain the presence of such sharp and intense band. Much weaker and broader feature at 990 cm^{-1} in the spectrum of *sdp*- VO_x/ZrO_2 reflects heterogeneity of the terminal V=O groups, typical of the two-dimensional oxovanadium surface clusters of relatively low crystallinity.

The differences in aggregation of surface vanadium species can also be revealed by EPR, using the V^{4+} ($3d^1$) ions, appearing in the *sdp*- VO_x/ZrO_2 and *imp*- VO_x/ZrO_2 samples, as a paramagnetic probe. The EPR spectra of both samples can be analyzed in terms of the supposition of two signals: a broad structureless one, due to magnetically interacting clustered species, and a narrow signal with the resolved hyperfine structure of isolated V^{4+} centers. From the computer simulation of the spectra recorded for the fresh samples (Fig. 2), the relative fraction of the isolated surface vanadium was found to be 28% for *imp*- VO_x/ZrO_2 and 48% for *sdp*- VO_x/ZrO_2 , whereas the fraction of the clustered oxovanadium species (including V_2O_5) was equal to 63 and 19%, respectively, indicating much better dispersion of vanadium in the *sdp*- VO_x/ZrO_2 sample.

The parameters of the broad ($\Delta B_{\text{pp}} \approx 17\text{ mT}$) EPR signal of the surface oxovanadium clusters ($g_{\parallel} = 1.952$ and $g_{\perp} = 1.979$ for *imp*- VO_x/ZrO_2 and $g_{\parallel} = 1.950$ and $g_{\perp} = 1.973$ for *sdp*- VO_x/ZrO_2) were almost insensitive to the preparation method. They remain in a good agreement with the parameters found previously for partially reduced vanadia [17]. The species containing magnetically isolated V^{4+} give rise to an axial EPR signal with the well-resolved eight-line hyperfine structure (due to ^{51}V with $I = 7/2$ and 100% natural abundance). The magnetic parameters, $g_{\parallel} = 1.930$, $g_{\perp} = 1.979$ and $|A_{\parallel}| = 18.56\text{ mT}$, $|A_{\perp}| = 6.12\text{ mT}$, for *imp*- VO_x/ZrO_2 and $g_{\parallel} = 1.925$, $g_{\perp} = 1.977$ and $|A_{\parallel}| = 17.96\text{ mT}$, $|A_{\perp}| = 6.45\text{ mT}$ for *sdp*- VO_x/ZrO_2 were found to be distinctly different, depending on the sample preparation method. Such signals, with $g_{\perp} > g_{\parallel}$ and $A_{\parallel} > A_{\perp}$, are characteristic of isolated vanadyl ions in a square pyramidal or tetragonally distorted octahedral coordination with approximate C_{4v} symmetry. The constituting ligands can be formed by the oxygens of the ZrO_2 matrix, adsorbed water molecules or hydroxyls bonded to vanadium [18]. The distortion of the surface vanadyl complex can be gauged by the factor $B = (g_{\parallel} - 2.0023)/(g_{\perp} - 2.0023)$ [18]. Substitution of the

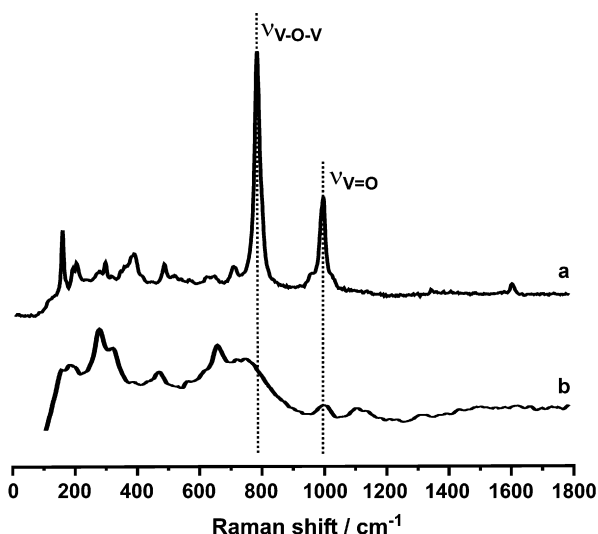


Fig. 1. Normalized Raman spectra of as prepared: (a) *imp*- VO_x/ZrO_2 and (b) *sdp*- VO_x/ZrO_2 samples, recorded at ambient conditions.

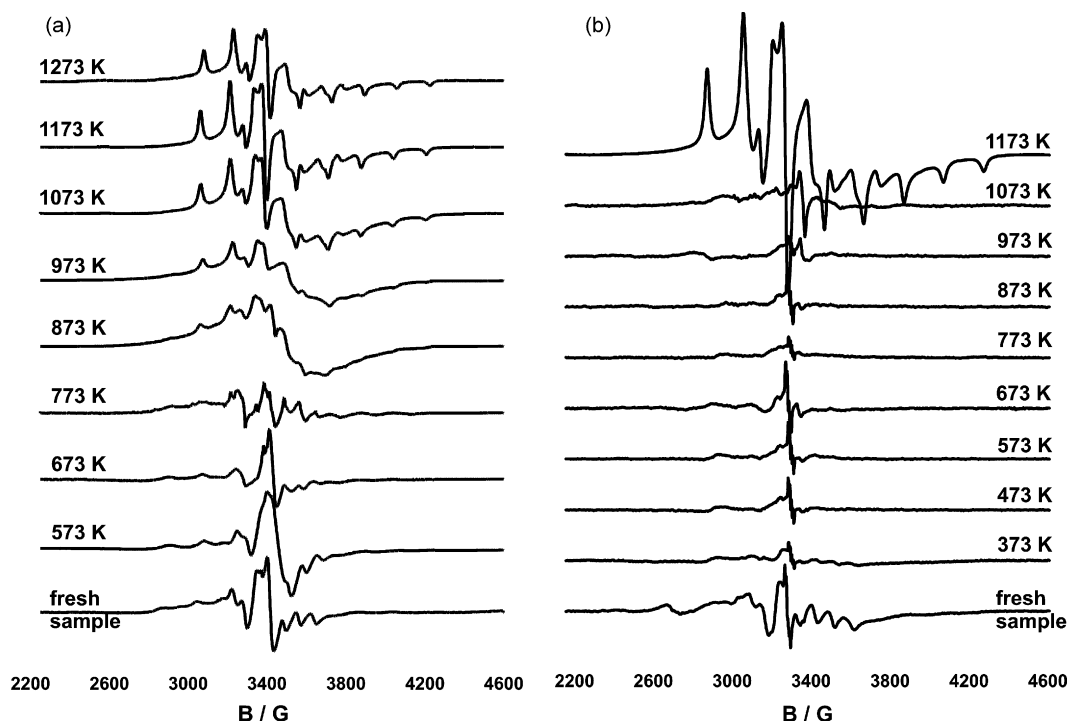


Fig. 2. X-band EPR spectra of: (a) *imp*-VO_x/ZrO₂ and (b) *sdp*-VO_x/ZrO₂ samples, recorded at 77 K before and after calcination at progressively increasing temperatures.

numerical values gives $B = 3.10$ for *imp*-VO_x/ZrO₂ and $B = 3.05$ for *sdp*-VO_x/ZrO₂, indicating a shortening of the terminal V=O bond and simultaneous weakening of the oxygen ligands in the equatorial plane for both samples, in comparison to those in V₂O₅ single crystals ($B = 4.9$) [19].

The sequence of the EPR spectra, recorded in the course of the variable temperature calcination is shown in Fig. 2. The axial signal, arising from the isolated V⁴⁺ surface centers, diminished with the increasing temperature and simultaneously a new orthorhombic signal with $g_{zz} = 1.8723$, $g_{xx} = 1.9759$, $g_{yy} = 1.9370$, $|A_{zz}| = 16.30$ mT, $|A_{xx}| = 5.59$ mT, $|A_{yy}| = 1.52$ mT, characteristic of V⁴⁺ isolated in the ZrO₂, gradually developed [13]. The threshold temperature, T_{th} , at which this signal emerged was distinctly different for *imp*-VO_x/ZrO₂ ($T_{th} = 873$ K) and *sdp*-VO_x/ZrO₂ ($T_{th} = 1073$ K) samples. It corresponds to dissolution of the isovalent V⁴⁺ ions in the ZrO₂ matrix, leading to formation of a substitutional V_xZr_{1-x}O₂ solid solution. This process is accompanied by a shrinkage of the *m*-ZrO₂ unit cell volume from $140.899 \pm 0.003 \text{ \AA}^3$ to $140.873 \pm 0.005 \text{ \AA}^3$, caused by the 13% difference in the V⁴⁺ and Zr⁴⁺ ionic radius, as inferred from Rietveld analysis of the XRD data. Changes in the EPR spectra observed during annealing of *imp*-VO_x/ZrO₂, suggest that formation of the solid solution ($T > 873$ K) precedes the phase transition from *t*-ZrO₂ to *m*-ZrO₂, taking place at $T > 973$ K. Consequently, the V⁴⁺ ions are dissolved in the tetragonal matrix giving rise to an axial signal, whereas for *sdp*-VO_x/ZrO₂, the opposite sequence occurs. The V⁴⁺ ions are dissolved in the monoclinic matrix at $T > 1073$ K (i.e., after the phase transition takes place), producing an orthorhombic EPR signal.

The initial disappearance (*sdp*-VO_x/ZrO₂) or weakening (*imp*-VO_x/ZrO₂) of the EPR signal due to the surface V⁴⁺ ions, in the course of the calcination in air, reflects their progressive oxidation to diamagnetic V⁵⁺ (3d⁰). Subsequent spontaneous reduction, necessary for incorporation of the vanadium into the bulk, was strongly related to the nature of oxovanadium surface species. The agglomerated species, prevailing in the case of *imp*-VO_x/ZrO₂, are more easily reduced than the isolated oxovanadium centers [20]. As a result, the evolution of the EPR spectra upon the heat treatment was much more dramatic than in the case of *sdp*-VO_x/ZrO₂. Thus, reducibility of the surface vanadium appears to be a key factor, controlling penetration of the vanadium ions into the zirconia matrix. Furthermore, there is a remarkable synergetic effect between the threshold temperature of V⁴⁺ migration towards the bulk and the phase transition of the tetragonal to monoclinic zirconia, in the case of the *imp*-VO_x/ZrO₂ samples. Such phase transition, was found not only to be accelerated in the presence of surface vanadium by *ca.* 300 K, but it also makes the V⁴⁺ migration easier. In case of the *sdp*-VO_x/ZrO₂ sample, because the well-dispersed vanadium ions are hardly reducible below 1073 K (Fig. 2b), their diffusion toward the bulk of the support was pronouncedly retarded. Interestingly, upon reaching the temperature of 1173 K it becomes quite rapid.

4. Conclusions

The way of V₂O₅ deposition onto tetragonal ZrO₂ support strongly influences the structure of surface oxovanadium species, their dispersion and dimensionality. Isolated and

clustered species were detected in the samples obtained by slurry deposition, whereas agglomerated oxovanadium and nanocrystalline V_2O_5 , dominated on the surface of samples prepared by slurry deposition. The dispersion state of surface vanadium strongly influences its reducibility and the threshold temperature of incorporation of the resultant V^{4+} ions into the bulk of the ZrO_2 matrix.

Acknowledgement

This work was financially supported by The Polish State Committee for Scientific Research (KBN) within the project 3 T09 147 26.

References

- [1] H.H. Kung, E.I. Ko, *Chem. Eng. J.* 64 (1996) 203–214.
- [2] J.A. Schwarz, C. Contescu, A. Contescu, *Chem. Rev.* 95 (1995) 477–510.
- [3] E. Hillerová, M. Zdražil, *Appl. Catal. A* 138 (1996) 13–26.
- [4] T. Klicpera, M. Zdražil, *Catal. Lett.* 58 (1999) 47–51.
- [5] A. Adamski, P. Jakubus, Z. Sojka, *Nukleonika* 51 (Suppl. 1) (2006) S27–S33.
- [6] R.A. Young, A.C. Larson, C.O. Paiva-Santos, *User's Guide to Program DBWS-9807a for Rietveld Analysis of X-ray and Neutron Powder Diffraction*, Schools of Physics, Georgia, Institute of Technology, Atlanta, GA, U.S.A. (2000).
- [7] T. Spalek, P. Pietrzyk, Z. Sojka, *J. Chem. Inf. Model.* 45 (2005) 18–29.
- [8] K.T. Jung, A.T. Bell, *J. Mol. Catal. A* 163 (2000) 27–42.
- [9] G. Katz, *J. Am. Ceram. Soc.* (1971) 531.
- [10] T. Hirata, *J. Phys. Chem. Solids* 56 (1995) 951–957.
- [11] K. Matsui, H. Suzuki, M. Ohgai, H. Arashi, *J. Ceram. Soc. Jpn. Int. Ed.* 98 (1990) 15–19.
- [12] T. Hirata, E. Asari, M. Kitajima, *J. Solid State Chem.* 110 (1994) 201–207.
- [13] A. Adamski, Z. Sojka, K. Dyrek, M. Che, *Solid State Ionics* 117 (1999) 113–122.
- [14] P. Clauws, J. Broeckx, J. Vennik, *Phys. Stat. Sol (b)* 131 (1985) 459–473.
- [15] M. Schraml, W. Fluhr, A. Wokaun, A. Baiker, *Ber. Bunsenges. Phys. Chem.* 93 (1989) 852–857.
- [16] T.R. Gilson, O.F. Bizri, N. Cheetham, *J. Chem. Soc., Dalton Trans.* (1973) 291–294.
- [17] Y. Kera, Y. Matsukaze, *J. Phys. Chem.* 90 (1986) 5752–5755.
- [18] V.K. Sharma, A. Wokaun, A. Baiker, *J. Phys. Chem.* 90 (1986) 2715–2718.
- [19] A. Adamski, Z. Sojka, K. Dyrek, M. Che, G. Wendt, S. Albrecht, *Langmuir* 15 (1999) 5733–5741.
- [20] S. Albrecht, G. Wendt, G. Lippold, A. Adamski, K. Dyrek, *Solid State Ionics* 101–103 (1997) 909–914.